

Accuracy of target volume and artifact reduction by optimal sorting methods of 4DCT image reconstruction on lung cancer radiotherapy in patients with mismatched pitch in irregular respiration

ความถูกต้องของปริมาตรก้อนเนื้อออกและการลดสิ่งแปลกปลอมบนภาพเอกซเรย์คอมพิวเตอร์แบบ 4 มิติด้วยวิธีการจัดเรียงข้อมูลภาพที่เหมาะสมสำหรับการฉายรังสีมะเร็งปอดในผู้ป่วยที่มีการตั้งค่าพิทช์ไม่สัมพันธ์กับรูปแบบการหายใจที่ไม่สม่ำเสมอ

Kamonchanok Nobphuek¹, Utumporn Puangragsa¹, Kullathorn Thephamongkhon¹, Patarapong Phasukkit², Sarut Puangragsa², Jiraporn Setakornnukul¹

¹Division of Radiation Oncology, Department of Radiology, Faculty of Medicine Siriraj Hospital, Mahidol University, Bangkok, Thailand.

²School of Engineering, King Mongkut's Institute of Technology Ladkrabang, Bangkok, Thailand.

Corresponding author:

Jiraporn Setakornnukul

Division of Radiation Oncology, Department of Radiology, Faculty of Medicine Siriraj Hospital, Mahidol University, 72-year building, basement, 2 Wanglang Road Bangkoknoi, Bangkok 10700, Thailand.

E-mail address: jiraporn.set@mahidol.ac.th

กมลชนก นอบเผือก¹, อุทุมพร พ่วงรักษา¹, กุลธร เทพมงคล¹, ภัทรพงษ์ ผาสุกกิจ², ศรุต พ่วงรักษา², จิราพร เสตกรณกุล¹

¹สาขาวิชารังสีรักษา ภาควิชารังสีวิทยา คณะแพทยศาสตร์ศิริราชพยาบาล มหาวิทยาลัยมหิดล

²คณะวิศวกรรมศาสตร์ สถาบันเทคโนโลยีพระจอมเกล้าคุณทหารลาดกระบัง

ผู้นิพนธ์ประสานงาน

จิราพร เสตกรณกุล

สาขาวิชารังสีรักษา ภาควิชารังสีวิทยา คณะแพทยศาสตร์ศิริราชพยาบาล มหาวิทยาลัยมหิดล

ตึก 72 ปี ชั้นใต้ดิน เลขที่ 2 ถนนวังหลัง แขวงศิริราช เขตบางกอกน้อย จังหวัดกรุงเทพมหานคร 10700

อีเมล: jiraporn.set@mahidol.ac.th

Submitted: Oct 13, 2023

Revised: Dec 24, 2023

Accepted: Jan 2, 2024

Abstract

Backgrounds: In four-dimensional computed tomography (4DCT), pitch estimates are initially selected before data acquisition. However, during data acquisition, it is observed that pitch values mismatch with the breathing period due to respiratory changes, leading to image artifacts. Addressing this issue requires the selection of an appropriate sorting method, especially for a group of patients in such cases who lack a standardized sorting protocol.

Objective: The study aims to determine the optimal 4DCT scan sorting method for patients with a set-up pitch not aligned with breathing period.

Materials and methods: The respiratory waveforms of 40 lung cancer patients were programmed into the CIRS dynamic thorax phantom, and data were acquired using a CT scanner. Subsequently, 4DCT scans were performed, and the appropriateness of the pitch values, which were set according to standard protocols, was assessed. Three sorting methods, namely phase-based, amplitude-based, and percent Pi-based, were evaluated for their impact on volume accuracy, shape, and the presence of artifacts on 4DCT image in terms of absolute volume difference (AVD), sphericity, and artifact score, respectively, specifically in six subjects with inappropriate parameter settings for acquisition data.

Results: Among the 40 patients studied, six respiratory waveforms had improper parameter settings. The volume of a spherical object for the respiratory phases of 0% and 50% showed similarities to the static volume in all three sorting methods, resulting in an AVD range of 0.18-0.29 cm³. The sphericity values of the three sorting methods with phases of 0% and 50% exhibited variations ranging from 0.001 to 0.003, and the artifacts exhibited a severity level close to 2. Therefore, the study recommended using the images at the 0% and 50% respiratory phase with all sorting methods for target contouring images in clinical practice, as they closely matched the static volume. The findings emphasize the importance of aligning pitch values with the breathing period during data acquisition to maintain image quality.

Conclusion: In patients with irregular breathing amplitude and a mismatch in respiratory rate and breathing period, phase-based or percent Pi-based sorting methods were preferably used for 4DCT reconstructions.

Keywords: Artifact, Four-dimensional computed tomography, Radiotherapy, Sorting, Tumor volume

บทคัดย่อ

หลักการและเหตุผล: การทำเอกซเรย์คอมพิวเตอร์แบบสปีดเลือกประมาณค่าพิทช์ก่อนเก็บข้อมูล ต่อมาขณะเก็บข้อมูลพบค่าพิทช์ไม่สัมพันธ์กับระยะเวลาการหายใจเนื่องจากการหายใจเปลี่ยนแปลงไปจึงเกิดสิ่งแปลกปลอมขึ้นบนภาพจำเป็นต้องแก้ไขปัญหานี้รวมไปถึงการเลือกใช้วิธีการจัดเรียงข้อมูลภาพที่เหมาะสมในกลุ่มผู้ป่วยกลุ่มนี้และยังไม่มีโปรโตคอลที่เป็นมาตรฐานสำหรับวิธีการจัดเรียงข้อมูลภาพ

วัตถุประสงค์: เพื่อกำหนดวิธีการจัดเรียงข้อมูลภาพในการทำเอกซเรย์คอมพิวเตอร์แบบสปีดที่เหมาะสมสำหรับผู้ป่วยที่มีการตั้งค่าพิทช์ไม่สัมพันธ์กับการหายใจ

วัสดุและวิธีการ: ข้อมูลสัญญาณการหายใจของผู้ป่วยมะเร็งปอด 40 คนใส่ลงหุ่นจำลองการหายใจ เก็บข้อมูลโดยเครื่องเอกซเรย์คอมพิวเตอร์แบบสปีด ประเมินความเหมาะสมของค่าพิทช์ซึ่งตั้งค่าตามโปรโตคอลมาตรฐานเลือกวิธีการจัดเรียงข้อมูลภาพ แบบเฟส แบบแอมพลิจูด และแบบเปอร์เซ็นต์หายใจ ประเมินความถูกต้องของปริมาตรรูปร่าง และสิ่งแปลกปลอมบนภาพ ในแง่ความแตกต่างของปริมาตรสัมบูรณ์ สภาพทรงกลม และให้คะแนนระดับสิ่งแปลกปลอมตามลำดับ โดยเฉพาะในผู้ป่วยที่มีการตั้งค่าพารามิเตอร์ที่ไม่เหมาะสมในการเก็บข้อมูล

ผลการศึกษา: จากผู้ป่วย 40 คน พบ 6 คนที่มีการตั้งค่าพารามิเตอร์ที่ไม่เหมาะสม ผลการศึกษาปริมาตรทรงกลม เฟสการหายใจที่ 0% และ 50% มีปริมาตรใกล้เคียงกับปริมาณทรงกลมขนาดจริงในการจัดเรียงข้อมูลภาพทั้งสามวิธี ผลของช่วงปริมาตรสัมบูรณ์ อยู่ที่ 0.18-0.29 ลูกบาศก์เซนติเมตร ค่าความเป็นทรงกลมทั้งสามวิธีที่เฟสการหายใจ 0% และ 50% มีความแปรผันตั้งแต่ 0.001 ถึง 0.003 และระดับความรุนแรงของสิ่งแปลกปลอมเข้าใกล้ 2 ดังนั้นจากการศึกษาครั้งนี้แนะนำให้เลือกใช้ภาพที่เฟสการหายใจ 0% และ 50% ในทั้งสามวิธีสำหรับการวัดขอบเขตก้อนมะเร็งในทางคลินิกเนื่องจากมีความใกล้เคียงกับปริมาตรจริง และควรตระหนักถึงความสำคัญของการตั้งค่าพิทช์ให้สอดคล้องกับระยะเวลาการหายใจในระหว่างเก็บข้อมูลเพื่อรักษาคุณภาพของภาพ

ข้อสรุป: ในผู้ป่วยที่มีแอมพลิจูดของการหายใจที่ไม่สม่ำเสมอ อัตราการหายใจและระยะเวลาการหายใจไม่ตรงกันควรใช้วิธีการจัดเรียงข้อมูลภาพแบบเฟสหรือแบบเปอร์เซ็นต์หายใจ สำหรับสร้างภาพ

คำสำคัญ: สิ่งแปลกปลอม, เอกซเรย์คอมพิวเตอร์แบบสปีด, รังสีรักษา, การจัดเรียงข้อมูลภาพ, ปริมาตรก้อนมะเร็ง

J Thai Assoc Radiat Oncol 2024; 30(1): R19 - R37

Introduction

The 4DCT (four-dimensional computed tomography) comprises the 3D CT dataset obtained from the CT scanner alongside the patient's respiratory signals acquired from an external surrogate device. These signals are recorded simultaneously or at corresponding timestamps with each respiratory cycle^[1, 2]. The data acquisition involves a slow couch movement characterized by a low pitch. In spiral mode, a low pitch value is necessary to capture each voxel of the patient's anatomy for an entire respiratory cycle^[3]. The maximum pitch depends on the patient's respiratory frequency and exceeding it can lead to motion artifacts. As a result, the pitch serves as a crucial parameter that requires careful consideration during a 4DCT scan. Particularly, configuring the pitch value unrelated to the breathing period can lead to image artifacts. Furthermore, according to Keall et al.^[4], it is recommended that the ratio of rotation time to pitch be equal to or exceeds the duration of the breathing period. This strategy ensures the acquisition of an adequate number of breathing cycles for a comprehensive 4DCT image and mitigates the risk of encountering data sufficiency condition (DSC).

In a practical scenario, certain patients encountered difficulties in maintaining a consistent respiratory pattern during 4DCT scans. The respiratory rate could change while the beam was active, leading to a disparity between

the predetermined pitch set before the 4DCT and the actual respiratory rate during the scan. Various approaches existed to address irregular breathing, including breathing-adapted 4DCT^[5-9] and the implementation of visual or audio feedback systems^[10]. These solutions demanded new software or hardware components and thorough intensive training. Another approach for solving this issue was the selection of an optimal sorting method for 4DCT data. There were three categorizations of sorting techniques: amplitude-based, phase-based, and Pi-based.

Currently, there is a lack of automated detection methods to identify instances where the set-up pitch is not aligned with the breathing period. Moreover, there is a shortage of established standard protocols or consensus for sorting data under such conditions. Consequently, this study aims to determine the most suitable sorting approach for addressing this scenario.

Material and method

Preparation of respiratory waveform data

The respiratory waveform data was collected from 40 lung cancer patients who received treatment at the radiotherapy division of Siriraj Hospital between 2018 to 2021. The data was obtained using the Somatom Confidence RT Pro scanner (Siemens Healthcare, Forchhiem, Germany), without utilizing the deep inspiration breath hold (DIBH) technique. The respiratory

waveform was recorded using dynamic thorax phantom model 008A (CIRS, Norfolk, Virginia, USA). In accordance with the requirements for retrospective studies, the concept and study design of this study were approved by Siriraj Institutional Review Board (study code: Si 035/2022).

4DCT acquisition

All 40 respiratory waveforms were programmed into the dynamic thorax phantom model 008A (CIRS, Norfolk, VA, USA) using an in-house wooden rod, as demonstrated in **Figure 1**. This wooden rod contained an oblique aluminum plate with a thickness of 2 mm and a spherical object with a diameter of 2 cm (tumor target), measured with a caliper. The aluminum plates were used to evaluate artifact severity, while the spheres displayed distortions in size and shape.

A 4DCT scan was performed using Siriraj Hospital's routine lung 4DCT protocol during the data acquisition process, employing the real-time position management (RPM) system (Varian Medical Systems, Palo Alto, CA, USA) for motion tracking. Then, the reference points in the respiratory signal data recorded via the RPM were adjusted using an in-house Python script (<https://github.com/bombonTH/SIRO-RPM-Peak-Correction>). The points stamped by the RPM, including the peaks and valleys of the respiratory signal, were corrected. This adjustment is crucial as these points serve as references for the reconstruction in the next step.

Acquisition parameters for the spiral 4DCT images were set as follows: 120 kV, 84 mAs, 350 mm FOV, 2 mm slice thickness, 0.5s rotation time, and B30F medium smooth kernel reconstruction filter. The 3DCT image dataset was synchronized with the RPM reference motion file. The scanner's rotation time and pitch were automatically determined by observing the breathing period on the RPM monitor in correlation with the selected range of estimated respiration rates on CT scanner.

Verification of the appropriateness of parameters during the data acquisition process

Calculate the appropriate rotation time per pitch value that corresponds to the breathing period. Afterward, verify that the rotation time per pitch value for each respiratory waveform exceeds the breathing period^[11], using the following formula:

$$\frac{\text{Gantry rotation time}}{\text{Pitch}} \geq \text{Breathing period}$$

The rotation time per pitch values can typically be obtained from the 4DCT scanner instruction manual in **Table 1**. In order to optimize 4DCT scans based on a patient's respiration rate, measured in breaths per minute (BPM), specific settings for rotation time and pitch are recommended. For patients with a respiration rate greater than 6 BPM, but not exceeding 9 BPM, a rotation time of 1 second with a pitch

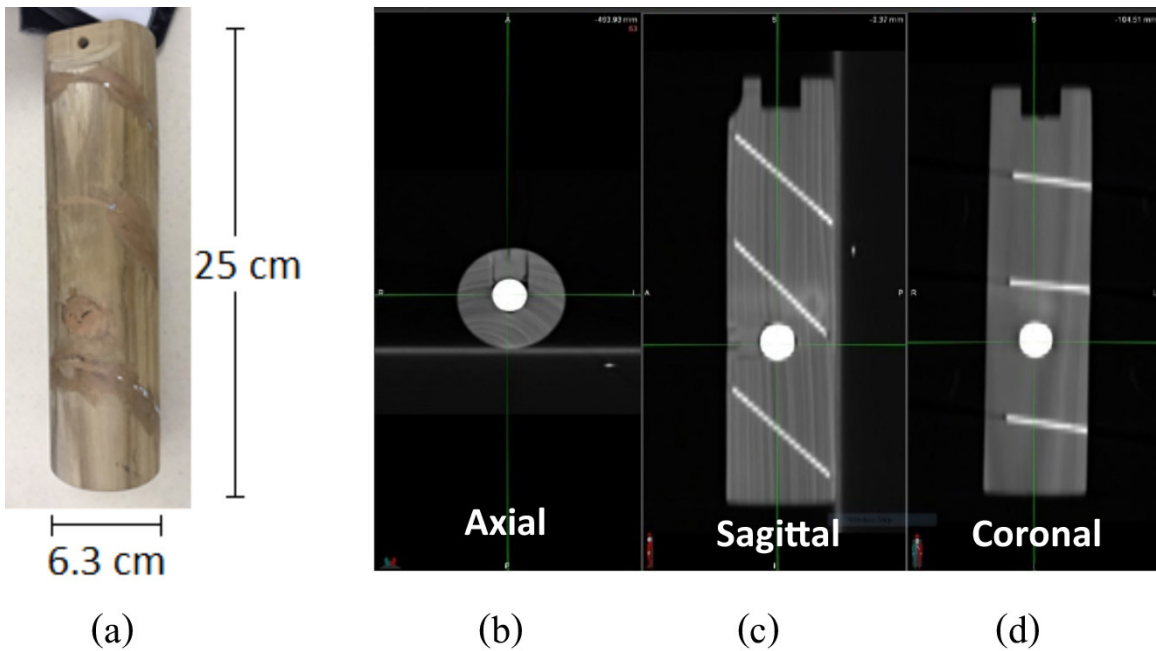


Figure 1 (a) The improvised in-house wooden rod is presented in three cross-sectional planes— (b) axial, (c) sagittal, and (d) coronal. The inside of the wooden rod contains an oblique aluminum slab with a thickness of 0.2 cm and a spherical object (marble) with a diameter of 2 cm, measured with a caliper.

of 0.09 is advised. This configuration results in a rotation time to pitch ratio of 11.11, which is suitable for breathing periods that range between 10 to 11.10 seconds. For those whose respiration rate exceeds 9 BPM but is no more than 12 BPM, the rotation time remains at 1 second, but the pitch is increased to 0.14. This adjustment leads to a rotation time to pitch ratio of 7.14, ideal for breathing periods between 6.67 and 7.13

seconds. Lastly, for patients with a respiration rate over 12 BPM, a shorter rotation time of 0.5 seconds and a pitch of 0.09 are recommended, yielding a rotation time to pitch ratio of 5.56, suitable for breathing periods of 5 to 5.54 seconds. These tailored settings are crucial for aligning the scanner's operation with the patient's breathing pattern, significantly enhancing the quality and accuracy of the 4DCT images.

Table 1 The estimated respiration time values of 4DCT scanner obtained from the instruction manual and the appropriate breathing period values.

Est. respiration time (BPM)	Rotation time (s)	Pitch	Rotation time/pitch	Breathing period (s)
6-9	1	0.09	11.11	10.00-11.10
>9-12	1	0.14	7.14	6.67-7.13
>12	0.5	0.09	5.56	5.00-5.55

Abbreviation: BPM= breaths per minute, Est. respiration time= Estimated respiration time

Subsequently, it is essential to verify the suitability of the estimated respiratory time selection in relation to the breathing period of the RPM. The breathing period value displayed on the RPM screen during the acquisition process serves as an indicator of the appropriateness of the parameter settings. In the context of this 4DCT scanner, the Somatom Confidence RT Pro scanner (Siemens Healthcare, Forchhiem, Germany) establishes a fixed rotation time per pitch value for each tap, as detailed in Table 1. Therefore, our focus lies in evaluating range of the breathing period in relation to the rotation time per pitch value. This involves analyzing datasets within groups of inappropriate acquisition parameters, with a tolerance of the mean breathing period ± 0.5 standard deviation taken into consideration.

Image sorting for 4DCT reconstruction

Following dynamic phantom scanning, images obtained under inadequate acquisition

parameters were categorized into ten phases using amplitude-based, phase-based, and percentage pi algorithms.

For the amplitude sorting, the acquired CT images are sorted based on the displacement. The breathing cycle is divided by the range of inhalation and exhalation into five equidistant steps from maximum to minimum. The amplitude sorting method in 4DCT presents an advantage in highlighting variations in physiological signals, offering insights into anatomical changes throughout the respiratory or cardiac cycle. However, its disadvantage lies in potential susceptibility to noise, as variations in amplitude may not always correlate precisely with anatomical motion.

In contrast, phase-based sorting, CT images are sorted based on the phase or relative timing within the patient's breathing cycle. The respiratory cycle is divided into the percentage of equal time points from peak to peak in each

respiratory cycle^[12]. The phase-based sorting method excels in providing a temporal perspective, but its drawback involves potential inaccuracies if the phase information is affected by irregularities or inconsistencies in physiological cycles.

Meanwhile, the percentage of Pi (percent Pi-based sorting), CT images are sorted based on the phase but use a different representation of the respiratory cycle. The respiratory cycle is represented in terms of pi (π), where 0% corresponds to 0π and 100% corresponds to 2π . The prominent point in this method is the position where 0% corresponds to the end inhalation, and 50% corresponds to the end exhalation position. The resulting image in this point will be the anatomical position corresponding to the actual breathing position of the patient. The percent Pi-based sorting method optimizes temporal resolution, yet its disadvantage lies in the complexity of implementation and potential challenges in maintaining synchronization due to the periodicity of 2π .

Evaluation of volume, shape, and artifact characteristics under inappropriate data acquisition parameters

Characteristics of breathing patterns under inappropriate data acquisition parameters were evaluated in terms of absolute volume difference (AVD), shape, and artifact in MIM software version 7.0 (MIMvista Corp., Cleveland, OH, USA) by using auto-segmented contour at 40 HU in ten phases (WW -362 HU and WL 1324 HU). The AVD was

calculated to evaluate the variation in volume for each sorting method. The AVD represents the volume difference between tumor volumes in each phase of the sorting method, compared to a static tumor in MIM software. The shape accuracy of the tumor is evaluated by the sphericity (Ψ), using the following formula.

$$\Psi = \frac{2^3 \sqrt{ab^2}}{a + \frac{b^2}{\sqrt{a^2 - b^2}} \ln\left(\frac{a + \sqrt{a^2 - b^2}}{b}\right)}$$

The sphericity measured semi-major (a) and semi-minor (b) axes^[13] as shown in **Figure 2**. The good sphericity should be close to 1^[14].

Furthermore, for artifact assessment, two evaluators assigned scores to the discrepancies observed in the intermediate aluminum slab within the 4DCT image shown in **Figure 3**. In cases where there were significant discrepancies in their assessments, a third expert was confirmed to provide a final determination. Artifacts in each sorting method were simultaneously evaluated on the sagittal plane at the same phase. None of the artifacts gives a 0 score, one artifact on the aluminum plate =1, two artifacts on the aluminum plate =2, and three artifacts on the aluminum plate = 3.

A statistical analysis comparing volume, shape, and image artifacts between three sorting types was tested using multilevel mixed-effects linear regression in Stata (Erlangen, Germany). The statistical significance was a p-value less than 0.05.

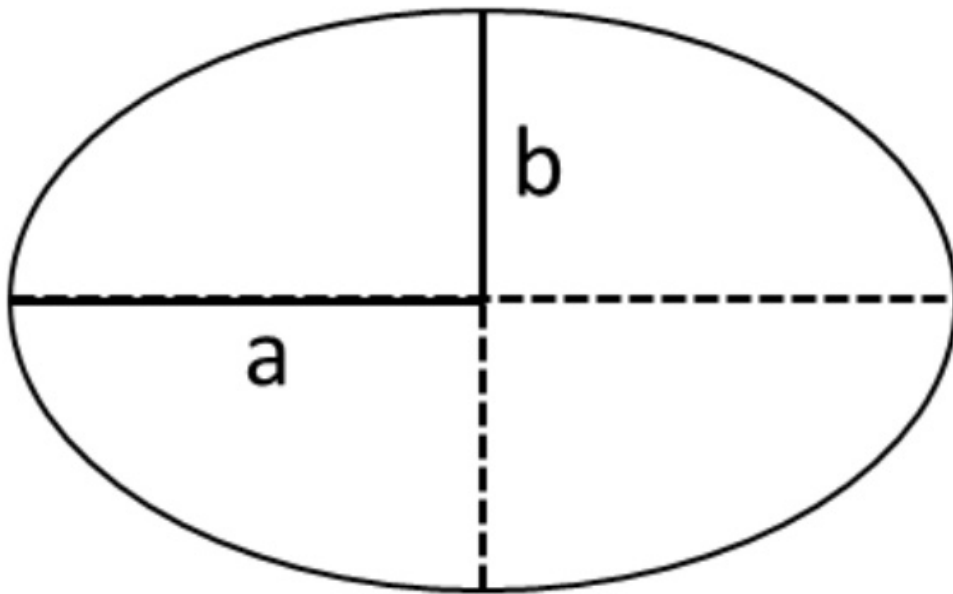


Figure 2 (a) The semi-major and (b) semi-minor axis of an ellipse.

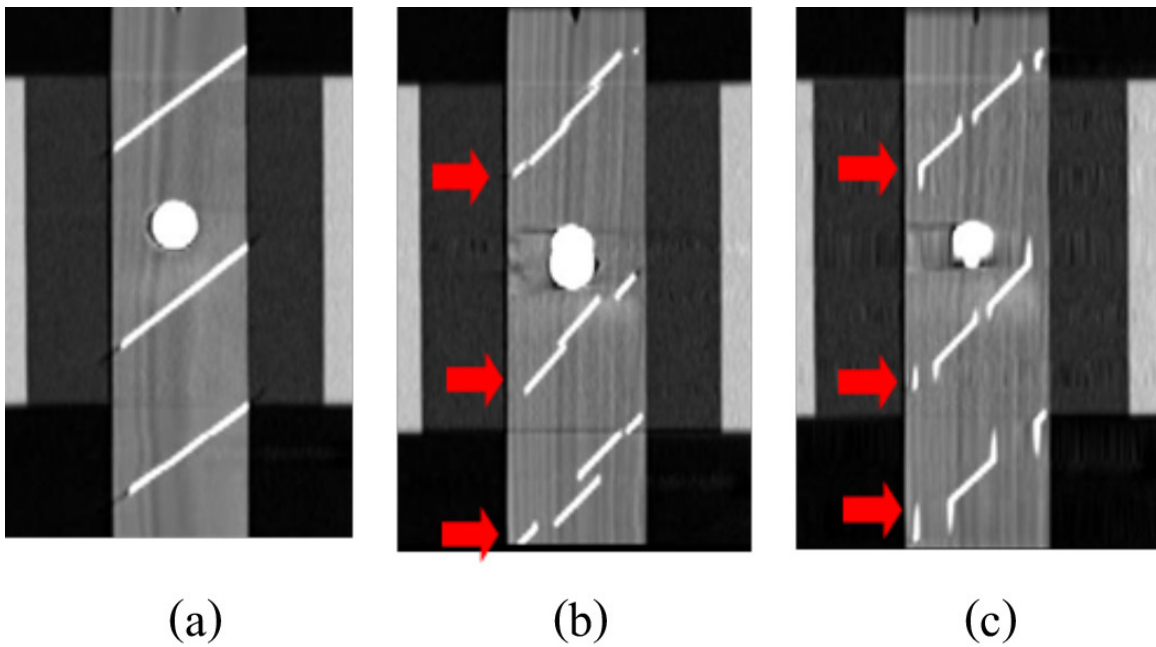


Figure 3 An example artifact found on the 4DCT image considering the anomaly of the aluminum slab: (a) No artifact, (b) and (c) Artifact on 4DCT images in the phantom, indicated by red arrows.

Results

Among the 40 patients studied, six cases had the rotation time per pitch value (7.14) shorter than the breathing period value plus 0.5 standard deviation (7.66 to 11.78) during the actual scan due to changes in the patient's respiratory rate during the scan. Therefore, these six patients were controlled in this study. These effects resulted in an inadequate amount of data for generating 4DCT images, as indicated in **Table 2**.

The study assessed the accuracy of volume, shape, and artifact in the respiratory waveforms of six respiratory waveforms with improper parameter settings or mismatched pitch in irregular respiration. Volume accuracy was assessed using AVD values, with amplitude-based, phase-based, and percent Pi-based methods yielding the values in the ranges of 0.18-1.23 cm³, 0.15-1.16 cm³, and 0.17-1.11 cm³, respectively

(**Figure 4**). Considering the volume (red circle) at the phase of 0% and 50% showed similarities to the static volume in all three sorting methods, resulting in an AVD range of 0.18-0.29 cm³ (**Table 3, Figure 4**). The 20% respiratory phase revealed no significant volume differences among the three imaging methods ($p > 0.05$).

The amplitude-based sorting method demonstrated significantly superior volume accuracy compared to the phase-based and percent Pi-based sorting methods at 10% respiratory phase (0.62 cm³, 1.16 cm³, and 1.11 cm³, respectively) (**Table 3**). Conversely, the phase-based and percent Pi-based sorting methods exhibited higher AVD values than the amplitude-based sorting method, particularly noticeable at respiratory phases 30% and 40%, with a statistically significant difference ($p < 0.001$) (**Table 3**)

Table 2 Inappropriate data acquisition parameters settings for 6 patients during scan 4DCT.

No. Patient	Pre-scan			During scan	Rot/pitch	Appropriate CT setting (Est. respiration time) (BPM)
	Breathing period (s) (Visualization)	Breathing period (s) ± 0.5 SD	(Est. respiration time) (BPM)	Breathing period (s) +0.5 SD		
PT01	9.0	11.07 ± 0.72	>9	11.78	7.14	>6
PT02	7.1	7.20 ± 0.46	>9	7.66	7.14	>6
PT03	7	6.97 ± 0.89	>9	7.86	7.14	>6
PT04	8.4	8.18 ± 0.59	>9	8.77	7.14	>6
PT05	7.1	6.91 ± 0.53	>9	7.44	7.14	>6
PT06	9.3	8.57 ± 0.81	>9	9.38	7.14	>6

Table 3 The absolute volume differences with mismatched pitch in irregular respiration.

Phase	Absolute Volume Difference			AB-PB (95%CI)	p-value	PB-Pi (95%CI)	p-value	AB-Pi (95%CI)	p-value
	AB±SD	PB±SD	Pi±SD						
0%	0.21±0.40	0.18±1.07	0.17±1.07	-0.03 (-0.63 to 0.57)	0.93	-0.01 (-0.61 to 0.59)	0.98	-0.04 (-0.64 to .56)	0.90
10%	0.62±0.29	1.16±1.04	1.11±1.05	0.54 (0.05 to 1.04)	0.03	-0.05 (-0.54 to 0.45)	0.86	0.50 (0.00 to 0.99)	0.05
20%	0.77±0.36	0.86±0.59	0.85±0.56	0.10 (-0.12 to 0.32)	0.37	-0.02 (-0.12 to 0.32)	0.37	0.08 (-0.14 to 0.30)	0.46
30%	1.18±0.70	0.78±0.64	0.77±0.63	-0.41 (-0.65 to -0.16)	<0.01	-0.01 (-0.25 to 0.24)	0.97	-0.41 (-0.66 to -0.17)	<0.01
40%	1.23±0.66	0.44±0.07	0.44±0.08	-0.79 (-1.18 to -0.40)	<0.01	0.00 (-0.39 to 0.39)	1.00	-0.79 (-1.18 to -0.40)	<0.01
50%	0.18±1.07	0.27±0.56	0.29±0.52	0.09 (-0.36 to 0.55)	0.69	0.02 (-0.44 to 0.47)	0.94	0.11 (-0.34 to 0.56)	0.64
60%	0.20±1.26	0.46±0.56	0.44±0.61	0.27 (-0.18 to 0.71)	0.24	-0.02 (-0.46 to 0.43)	0.94	0.25 (-0.19 to 0.69)	0.27
70%	0.35±1.16	0.62±0.96	0.60±0.94	0.28 (-0.32 to 0.88)	0.36	-0.03 (-0.63 to 0.57)	0.93	0.25 (-0.35 to 0.85)	0.41
80%	0.54±0.68	0.46±1.29	0.46±1.26	-0.09 (-0.50 to 0.32)	0.67	0.00 (-0.41 to 0.41)	0.99	-0.08 (-0.49 to 0.32)	0.68
90%	0.71±0.43	0.15±1.42	0.19±1.38	-0.56 (-1.17 to 0.04)	0.07	0.04 (-0.57 to 0.64)	0.91	-0.53 (-1.14 to 0.08)	0.09

Abbreviation: AB= Amplitude-based sorting, PB= Phase-based sorting, Pi= Percent Pi-based sorting

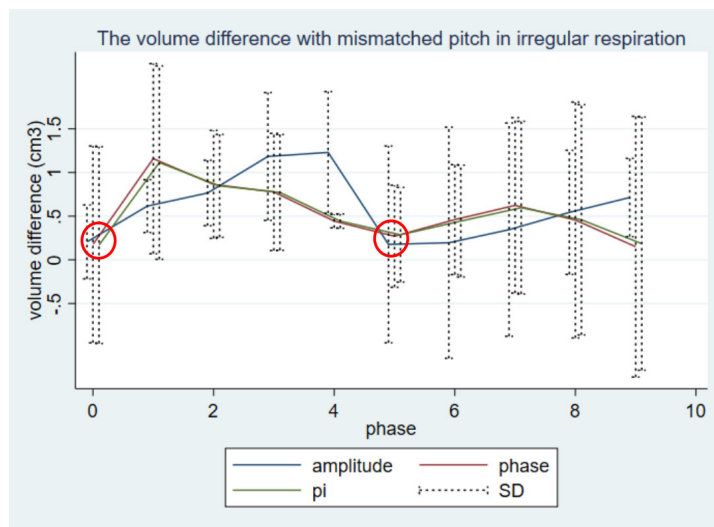


Figure 4 The AVD including amplitude-based (blue line), phase-based (red line), and percent Pi-based (green line) sorting with mismatch pitch in irregular respiration. The red circle at the phase of 0% and 50% showed similarities to the static volume in all three sorting methods. Dotted lines represent data within standard deviations.

Additionally, when assessing shape differences, which are evaluated through sphericity values, a value close to 1 indicates that the shape closely resembles the ideal roundness. As depicted in **Table 4**, the sphericity values of the three sorting methods demonstrated differences not exceeding 0.02. Particularly, during the 0% and 50% respiratory phases, the sphericity exhibited variations ranging from 0.001 to 0.003. Both the phase-based and percent Pi-based sorting methods displayed sphericity in a similar direction, with no statistically significant differences noted ($p>0.05$).

In **Figure 5**, the phase-based and percent Pi-based sorting methods are closer to reality shape than the amplitude-based sorting method

observed at respiratory phase 30% to 70%. However, at the 20% respiratory phase, the sphericity appeared similar for all three sorting methods. Even though there were no significant differences in AVD during this phase, it's notable that the sphericity of the amplitude-based sorting method significantly differed from that of the phase-based and percent Pi-based methods ($p=0.02$ and $p=0.04$, respectively).

For the artifacts present in the 4DCT image, assessed through the continuity of the aluminum middle slab, the resulting artifacts exhibited a severity level close to 2 (two artifacts on the aluminum plate), as depicted in **Figure 6**. However, the artifact severity did not exhibit a correlation with either volume or sphericity.

Table 4 The sphericity differences with mismatch pitch in irregular respiration.

Phase	Absolute Volume Difference			AB-PB (95%CI)	p-value	PB-Pi (95%CI)	p-value	AB-Pi (95%CI)	p-value
	AB	PB	Pi						
	0%	0.995	0.992						
10%	0.998	0.992	0.993	-0.006 (-0.012 to -0.001)	0.033	0.001 (-0.004 to 0.007)	0.675	-0.005 (-0.010 to 0.001)	0.086
20%	0.992	0.979	0.981	-0.013 (-0.024 to -0.002)	0.020	0.002 (-0.009 to 0.013)	0.774	-0.011 (-0.023 to 0.000)	0.041
30%	0.987	0.996	0.997	0.009 (0.002 to 0.016)	0.010	0.001 (-0.006 to 0.008)	0.822	0.010 (0.003 to 0.017)	0.005
40%	0.993	0.995	0.995	0.002 (-0.004 to 0.009)	0.513	-0.001 (-0.007 to 0.006)	0.877	0.002 (-0.005 to 0.008)	0.618
50%	0.992	0.995	0.995	0.003 (-0.004 to 0.010)	0.360	0.000 (-0.007 to 0.007)	0.984	0.003 (-0.004 to 0.010)	0.371
60%	0.991	0.997	0.997	0.006 (0.002 to 0.010)	0.007	-0.001 (-0.005 to 0.004)	0.777	0.005 (0.001 to 0.010)	0.016
70%	0.988	0.997	0.996	0.009 (-0.001 to 0.019)	0.095	-0.001 (-0.011 to 0.009)	0.900	0.008 (-0.002 to 0.018)	0.122
80%	0.989	0.992	0.991	0.002 (-0.006 to 0.011)	0.594	0.000 (-0.009 to 0.008)	0.923	0.002 (-0.007 to 0.011)	0.663
90%	0.997	0.990	0.991	-0.007 (-0.013 to -0.001)	0.021	0.000 (-0.005 to 0.006)	0.870	-0.006 (-0.012 to -0.001)	0.033

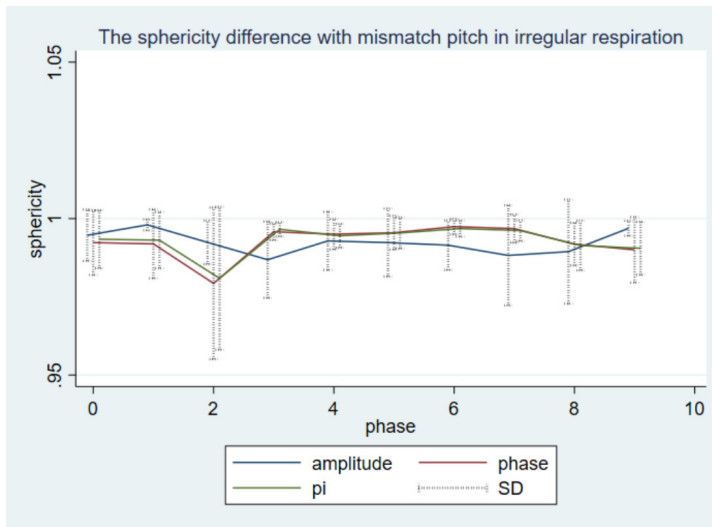


Figure 5 The sphericity difference including amplitude-based (blue line), phase-based (red line), and percent Pi-based (green line) sorting with mismatch pitch in irregular respiration. Dotted lines represent data within standard deviations.

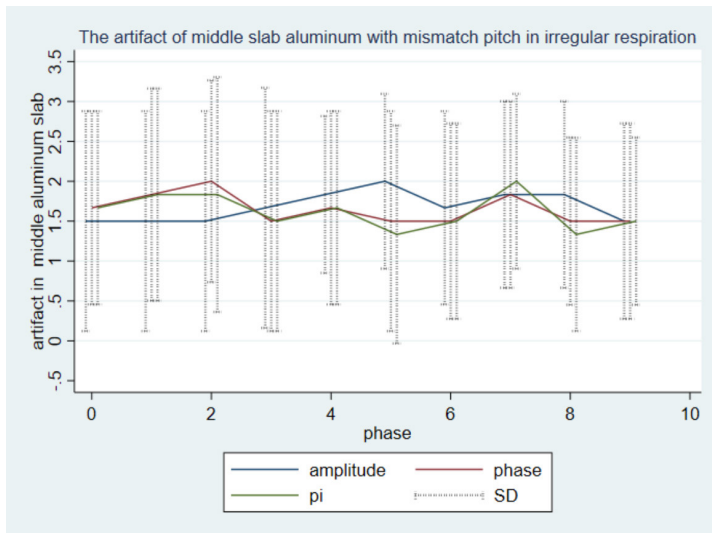


Figure 6 The artifact in middle slab aluminum including amplitude-based (blue line), phase-based (red line), and percent Pi-based (green line) sorting with mismatch pitch in irregular respiration. Dotted lines represent data within standard deviations.

Furthermore, when examining the phase-based and percent Pi-based sorting methods in **Table 5**, it was observed that at the 0% respiratory phase, there were 1.18 times more artifacts compared to the amplitude-based sorting method. For the 50% respiratory phase, the artifacts were 0.61 and 0.51 times less than the amplitude-based sorting method, respectively. Nonetheless, the artifacts identified by the three sorting methods exhibited no statistically significant differences, except during the 20% respiratory phase. Notably, during this phase, both the phase-based and percent Pi-based sorting methods displayed a higher artifact, with values 1.65 and 1.4 times greater than the amplitude-based method, respectively ($p=0.22$).

Discussion

After an examination of three sorting techniques employing the 4DCT scanner, it was determined that when acquisition parameters were improperly configured, none of the sorting methods yielded favorable outcomes in either amplitude-based, phase-based or percent Pi-based sorting. This significantly impacts the amplitude-based sorting method due to its reliance on precise amplitude-level positioning for sorting. Concurrently, both phase-based sorting and percent-Pi sorting exhibit comparable results.

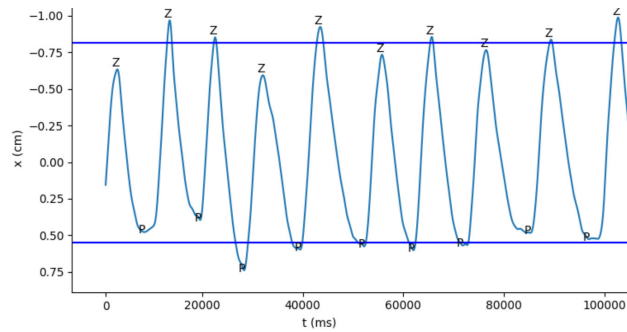
Furthermore, the presence of interpolated or incomplete artifacts was attributed to a respiratory waveform characterized by a

breathing period value shorter than the rotation time per pitch. For example (**Figure 7a**), the slow respiratory rate was 5.42, indicating a reduced number of cycles. Moreover, an incorrect estimation of the respiratory rate occurred, involving the selection of a rate exceeding 9 BPM instead of the suitable rate, which should have been greater than 6 BPM. This error became evident when reviewing the stack bar CT for each phase within the three sorting methods, as presented in **Figures 7b-7d**. Typically, the stack interval in sorting takes 250ms per bar, so selecting a fast respiratory rate instead of a slower one, resulted in a significant expansion of the data range. This discrepancy reconstruction method led to data interpolation due to missing information between stacks in all three sorting methods especially in amplitude-based sorting. Nevertheless, it's crucial to consider the rotation per pitch to prevent missing information when using the amplitude-based sorting method. Missing data can lead to interpolation and compensation for absent respiratory phases, resulting in image blurriness, elongation, and incompleteness.

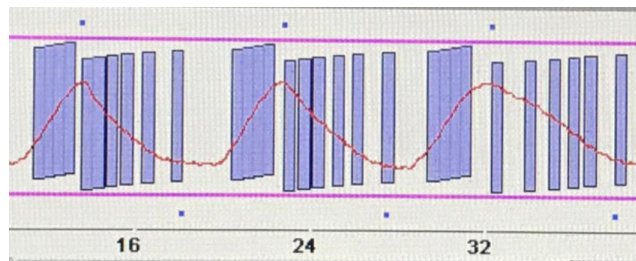
The upper portion of the volume appears elongated and truncated, leading to an increase in AVD. Consequently, severe artifacts are observed in the anatomical images on the 4DCT image of the patient, characterized by image blurring and missing anatomical details, as illustrated in **Figure 8**. Consequently, the contour delineation does not encompass the tumor.

Table 5 Artifact of middle slab aluminum with mismatch pitch in irregular respiration.

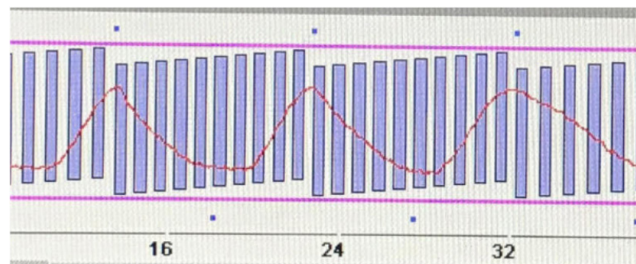
Phase	Odd ratio (95%CI, p-value)	Global p-value
0%: Amplitude	Reference	
Phase	1.18 (0.93-1.51, 0.18)	0.301
Pi	1.18 (0.93-1.51, 0.18)	
10%: Amplitude	Reference	
Phase	1.40 (1.03-1.90, 0.034)	0.050
Pi	1.40 (1.03-1.90, 0.034)	
20%: Amplitude	Reference	
Phase	1.65 (1.15-2.37, 0.007)	0.022
Pi	1.40 (0.97-2.00, 0.07)	
30%: Amplitude	Reference	
Phase	0.85 (0.66-1.08, 0.18)	0.301
Pi	0.85 (0.66-1.08, 0.18)	
40%: Amplitude	Reference	
Phase	0.85 (0.66-1.08, 0.18)	0.301
Pi	0.85 (0.66-1.08, 0.18)	
50%: Amplitude	Reference	
Phase	0.61 (0.36-1.02, 0.061)	0.864
Pi	0.51 (0.30-0.87, 0.012)	
60%: Amplitude	Reference	
Phase	0.85 (0.42-1.70, 0.639)	0.770
Pi	0.85 (0.42-1.70, 0.639)	
70%: Amplitude	Reference	
Phase	1.00 (0.59-1.69, 1.000)	0.235
Pi	1.18 (0.7-1.99, 0.532)	
80%: Amplitude	Reference	
Phase	0.72 (0.40-1.29, 0.265)	1.000
Pi	0.61 (0.34-1.09, 0.095)	
90%: Amplitude	Reference	
Phase	1.00 (0.69-1.46, 1.00)	0.864
Pi	1.00 (0.69-1.46, 1.00)	



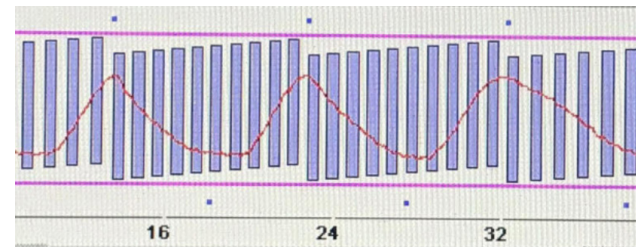
(a)



(b)



(c)



(d)

Figure 7 The impact of shallow or flat breathing on the respiratory waveform (a) and presents the stack bar CT images sorted by phase in the (b) amplitude-based, (c) phase-based, and (d) Pi-based sorting methods.

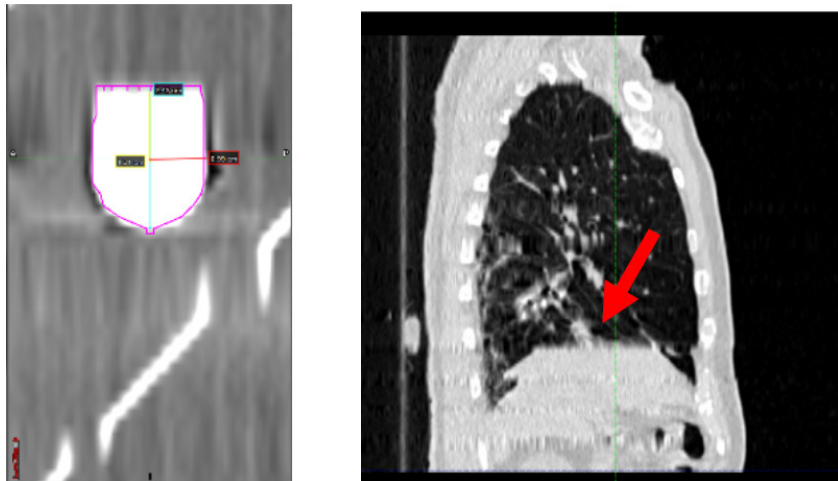


Figure 8 The presented artifact in the phantom (left) correlated with the patient (right) in the sagittal plane.

Respiratory waveforms, featuring low amplitudes, particularly in the amplitude-based sorting method, rendered it challenging to determine the phase position, leading to missing data. Li H et al.^[15] revealed similar findings where irregular breathing patterns resulted in a smaller volume in amplitude-based sorting method compared to phase-based sorting method, leading to image artifacts. Furthermore, Hilgers G et al.^[3] was associated with an inappropriate pitch value with breathing frequency, particularly when the selected estimated respiratory time does not correspond to the breathing period. Thus, it is recommended to appropriately adjust the rotation time per pitch, following the guidance of Keall PJ et al.^[4], to ensure a sufficient amount of cycle data for sorting and to prevent missing data.

One limitation of this research involves the evaluation of artifacts aimed at reducing interobserver variability. To address this limitation, a third party was employed to determine artifact scores. However, it's important to note that this method may not be universally applicable. Additionally, it's worth mentioning that this assessment solely focuses on the continuity of the aluminum slab and does not take into account elongation or curvature.

In practical implementations in improper acquisition parameter settings, it's crucial to assess the accuracy of respiratory volume. Therefore, in clinical practice when utilizing 4DCT images, it is advisable for target contouring to rely on respiratory phases at 0% and 50% since shown target volumes were closest to static volume (Figure 4). Additionally, it's import-

ant to avoid using Maximum Intensity Projection (MIP) images for contouring, as combining artifacts present in all phases can result in significant errors. Furthermore, it's essential to ensure the regularity of breathing and match the breathing period to the pitch value during data acquisition.

Conclusion

In clinical practice, when a patient has difficulty with regular breathing during a 4DCT scan, radiologists often utilize phase-based or percent Pi-based sorting methods to accurately ascertain the size and shape of a tumor. This technique is beneficial even if a patient is hesitant to undergo multiple 4DCT scans, as it effectively reduces artifacts, especially in phases 0% and 50%. During these phases, radiologists are typically able to more precisely evaluate the extent of the tumor.

Furthermore, oncologists can combine data from phases 0% and 50%, which correspond to the end-inhale and end-exhale phases, respectively, to calculate the range of tumor movement during treatment. Nonetheless, the ideal approach is to train patients in consistent breathing techniques prior to conducting the 4DCT to achieve the highest quality results.

For patients with irregular breathing amplitude and a discrepancy between respiratory rate and breathing period, phase or percent Pi-based sorting methods are recommended for 4DCT reconstruction in clinical settings. Additionally, radiotherapists should carefully select the rotation time per pitch value that aligns with the patient's breathing period. This choice of the appropriate auto pitch at the CT scanner is crucial for enhancing image quality.

References

1. Pan T. Comparison of helical and cine acquisitions for 4D-CT imaging with multislice CT. 2005;32:627-34.
2. Caines R, Sisson NK, Rowbottom CG. 4DCT and VMAT for lung patients with irregular breathing. J Appl Clin Med Phys 2022;23:e13453.
3. Hilgers G, Nuver T, Minken ACMP. Helical 4D CT pitch management for the Brilliance CT Big Bore in clinical practice. J Appl Clin Med Phys 2015;16:389-98.
4. Keall PJ, Starkschall G, Shukla H, Forster KM, Ortiz V, Stevens C, et al. Acquiring 4D thoracic CT scans using a multislice helical method. Phys in Med 2004;49: 2053-67.
5. Werner R, Hofmann C, Mücke E, Gauer T. Reduction of breathing irregularity-related motion artifacts in low-pitch spiral 4D CT by optimized projection binning. J Radia Oncol 2017;12:1-8.

6. Werner R, Sentker T, Madesta F, Gauer T, Hofmann C. Intelligent 4D CT sequence scanning (i4DCT): concept and performance evaluation. *Med Phys* 2019;46:3462-74.
7. Rietzel E, Chen GT. Improving retrospective sorting of 4D computed tomography data. *Med Phys* 2006;33:377-9.
8. Li R, Lewis JH, Cervino LI, Jiang SB, Biology. 4D CT sorting based on patient internal anatomy. *Phys Med Biol* 2009;54: 4821-33.
9. Freislederer P, Heinz C, von Zimmermann H, Gerum S, Roeder F, Reiner M, et al. Clinical workflow optimization to improve 4DCT reconstruction for Toshiba Aquilion CT scanners. *Z Med Phys* 2018; 28:88-95.
10. Pollock S, O'Brien R, Makhija K, Hegi-Johnson F, Ludbrook J, Rezo A, et al. Audiovisual biofeedback breathing guidance for lung cancer patients receiving radiotherapy: a multi-institutional phase II randomised clinical trial. *BMC cancer* 2015;15:1-8.
11. Keall PJ, Starkschall G, Shukla H, Forster KM, Ortiz V, Stevens C, et al. Acquiring 4D thoracic CT scans using a multislice helical method. *Phys Med Biol* 2004;49: 2053-67.
12. Wink N, Panknin C, Solberg TD. Phase versus amplitude sorting of 4D-CT data. *J Appl Clin Med Phys* 2006;7:77-85.
13. Wikipedia contributors. Sphericity: Wikipedia, The Free Encyclopedia.; [updated 21 October 2023; cited 2022 12 October 2022]. Available from: <https://en.wikipedia.org/w/index.php?title=Sphericity&oldid=1177772003>.
14. Zheng J, Hryciw RD. Traditional soil particle sphericity, roundness and surface roughness by computational geometry. *Geotechnique* 2015;65:494-506.
15. Li H, Noel C, Garcia-Ramirez J, Low D, Bradley J, Robinson C, et al. Clinical evaluations of an amplitude-based binning algorithm for 4DCT reconstruction in radiation therapy. *Med Phys* 2012;39: 922-32.